Large-scale quantum computation in an anharmonic linear ion trap

2009 EPL 86 60004

(http://iopscience.iop.org/0295-5075/86/6/60004)

A Letters Journal Exploring the Frontiers of Physics

June 2009

EPL, **86** (2009) 60004
doi: 10.1209/0295-5075/86/60004

www.epljournal.org

Large-scale quantum computation in an anharmonic linear ion trap

G.-D. Lin[1(a)], S.-L. Zhu[1,2], R. Islam[3], K. Kim[3], M.-S. Chang[3], S. Korenblit[3], C. Monroe[3] and L.-M. Duan[1]

[1] *FOCUS Center and MCTP, Department of Physics, University of Michigan - Ann Arbor, MI 48109, USA*
[2] *LQIT and ICMP, Department of Physics, South China Normal University - Guangzhou, China*
[3] *Joint Quantum Institute, University of Maryland and National Institute of Standards and Technology College Park, MD 20742, USA*

received 27 February 2009; accepted in final form 3 June 2009
published online 9 July 2009

PACS 03.67.Lx – Quantum computation architectures and implementations
PACS 32.80.Qk – Coherent control of atomic interactions with photons
PACS 03.67.Pp – Quantum error correction and other methods for protection against decoherence

Abstract – We propose a large-scale quantum computer architecture by more easily stabilizing a single large linear ion chain in a very simple trap geometry. By confining ions in an anharmonic linear trap with nearly uniform spacing between ions, we show that high-fidelity quantum gates can be realized in large linear ion crystals under the Doppler temperature based on coupling to a near-continuum of transverse motional modes with simple shaped laser pulses.

Trapped atomic ions remain one of the most attractive candidates for the realization of a quantum computer, owing to their long-lived internal qubit coherence and strong laser-mediated Coulomb interaction [1–4]. Various quantum gate protocols have been proposed [1,5–9] and many have been demonstrated with small numbers of ions [4,10–14]. The central challenge now is to scale up the number of trapped ion qubits to a level where the quantum behavior of the system cannot be efficiently modeled through classical means [4]. The linear rf (Paul) trap has been the workhorse for ion trap quantum computing, with atomic ions laser-cooled and confined in 1D crystals [1–4] (although there are proposals for the use of 2D crystals in a Penning trap [15] or array of microtraps [6]). However, scaling the linear ion trap to interesting numbers of ions poses significant difficulties [2,4]. As more ions are added to a harmonic axial potential, a structural instability causes the linear chain to buckle near the middle into a zigzag shape [16,17], and the resulting low-frequency transverse modes and the off-axis rf micromotion of the ions makes gate operation unreliable and noisy. Even in a linear chain, the complex motional mode spectrum of many ions makes it difficult to resolve individual modes for quantum gate operations, and to sufficiently laser cool many low-frequency modes. One promising approach is to operate with small linear ion chains and multiplex the system by shuttling ions between multiple chains through a maze of trapping zones, but this requires complicated electrode structures and exquisite control of ion trajectories [2,18].

In this paper, we propose a new approach to ion quantum computation in a large linear architecture that circumvents the above difficulties. This scheme is based on several ideas. First, an anharmonic axial trap provided by static electrode potentials can stabilize a single linear crystal containing a large number of ions. Second, tightly confined and closely spaced transverse phonon modes can mediate quantum gate operations in a large architecture [19], while eliminating the need for single-mode resolution and multimode sideband cooling. Third, gate operations on the large ion array exploit the local character of the laser-induced dipole interaction that is dominated by nearby ions only. As a result, the complexity of the quantum gate does not increase with the size of the system, and the gates can be performed in parallel on ions in different locations of the chain.

The proposed ion architecture is illustrated in fig. 1. It is a large linear array where the strong confinement in the transverse (x, y) direction is provided by the ponderomotive Paul trap with an effective potential of the form $V(x, y) = (m\omega_x^2 x^2 + m\omega_y^2 y^2)/2$, where m is the mass of each ion. The ions are initially Doppler cooled, with a number of ions at the edges of the chain continuously Doppler cooled in order to overwhelm any heating that

(a) E-mail: guindarl@umich.edu

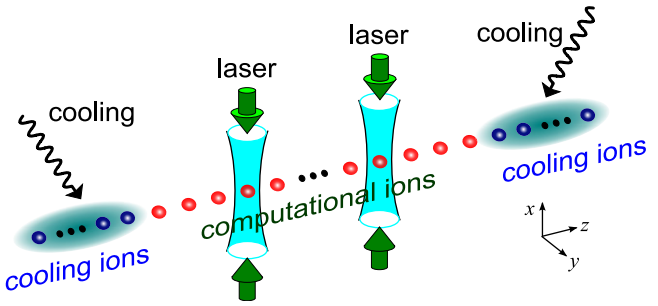

Fig. 1: (Color online) Linear architecture for large-scale quantum computation, where lasers address individual ions and couple to local modes of the ions, while the edge ions are continuously Doppler laser-cooled. In a large ion chain, more efficient sympathetic cooling could be achieved with cooling ions sparsely distributed in the ion chain.

occurs during the gate operation. The middle portion and majority of the ion chain is used for quantum computation. Given an appropriate axial static potential $V(z)$ from the axially segmented electrodes, we assume these computational ions are distributed nearly uniformly, with a neighboring distance of about $\sim 10\,\mu$m. This enables efficient spatial addressing with focused laser beams along the transverse direction for quantum gate operations.

When the axial potential takes the conventional harmonic form $V(z) = m\omega_z^2 z^2/2$, the ion array is subject to the well-known zigzag transition unless the trap anisotropy is at least $\omega_{x,y}/\omega_z > 0.77N/\sqrt{\log N}$ [2,17,20], where N is the number of ions. As N becomes large, this structural instability occurs first at the minimal distance at the trap center due to the spatial inhomogeneity of the ion distribution. When the ions under a similar trap anisotropy are instead uniformly spaced by neighboring distance d_0, it is easy to see that the linear structure is always stable even for an infinite chain so long as $\omega_{x,y}^2 > 7\zeta(3)e^2/(2md_0^3) \approx 4.2e^2/(md_0^3)$, where $\zeta(l)$ is the Reimann zeta function and e is the charge of each ion. Therefore, a large linear structure can be more easily stabilized so long as static potentials from the trap electrodes are designed to accommodate equally spaced ions. The uniformity of the distribution is critical for scaling because the minimum ion spacing can be kept constant to avoid the zigzag transition, while at the same time the maximum ion spacing does not grow, as is required for operating entangling gates efficiently across the whole chain, as described below.

To illustrate the general method, here we consider an explicit example with a quartic potential $V(z) = \alpha_2 z^2/2 + \alpha_4 z^4/4$ that can be realized with a simple five-segment electrode geometry as shown in fig. 2(a). Under a quartic trap $V(z)$, the axial equilibrium position z_i of the i-th ion can be obtained by solving the force balance equations $\partial U/\partial z_i = 0$, where $U = \sum_i [V(z_i) + V(x,y)] + \sum_{i<j} e^2/|\mathbf{r}_i - \mathbf{r}_j|$ is the overall potential including the ions' mutual interactions. We optimize the dimensionless ratio $B = |\alpha_2/e^2|^{2/3}(\alpha_2/\alpha_4)$ characterizing the axial potential to produce a nearly uniformly spaced crystal. To be concrete, we consider an array of 120 ions, with 10 ions at each edge continuously laser cooled and 100 qubit ions in the middle for coherent quantum gate operation. We solve the equilibrium positions of all the ions under $V(z)$ and minimize the variance in ion spacing $s_z = \sqrt{\frac{1}{100}\sum_{i=11}^{110}\left(\Delta z_n - \overline{\Delta z_n}\right)^2}$ for the qubit ions, where Δz_n is the distance between the n-th and $(n+1)$th ion in the chain and $\overline{\Delta z_n}$ denotes its average. The variance in spacing is shown in fig. 2(b) as a function of the parameter B. The value of s_z is fairly insensitive to B and reaches a minimum when $B \approx -6.1$. Here, the distribution of ion spacing z_n is shown in fig. 2(c), which is remarkably homogeneous for the qubit ions even though we have optimized just one control parameter: $s_z/\overline{\Delta z_n}$ deviates by only 3% over the entire crystal. In this configuration, if we take $\overline{\Delta z_n} = 10\,\mu$m for atomic Yb^+ ions, we only need a transverse center-of-mass frequency $\omega_{x,y}/2\pi > 221$ kHz to stabilize the linear structure. In this paper, we actually

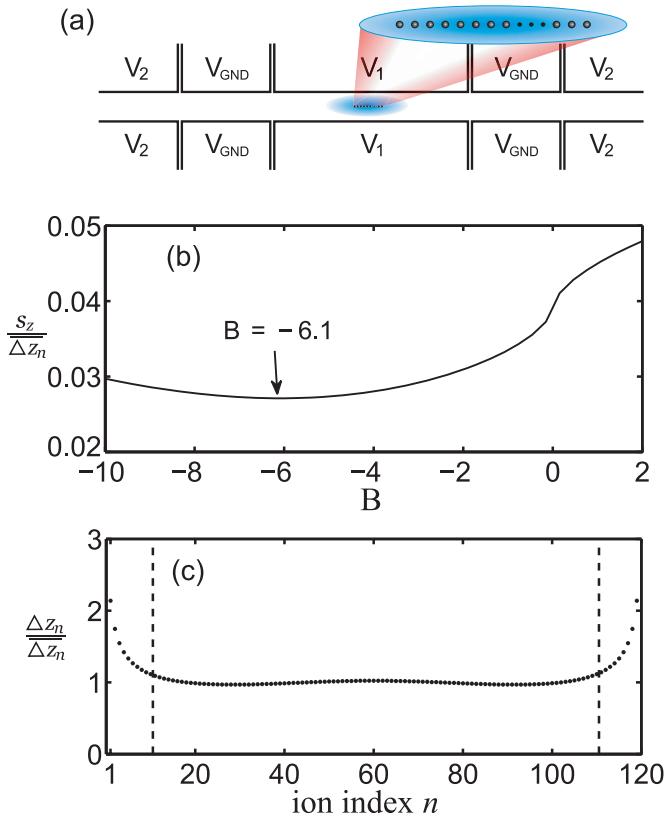

Fig. 2: (Color online) (a) Sample five-segment linear ion trap with voltages V_i $(i = 1, 2)$ to produce a quartic axial potential. The ions are confined in the central segment. (b) The variance of the ion spacings s_z in a linear quartic trap as a function of the trap parameter B that characterizes the ratio of quadratic to positive-quartic nature of the potential. (c) The distribution of the ion spacing at the optimum value $B = -6.1$. The computational ions are within the dashed lines, where the spacing is essentially uniform.

take $\omega_x/2\pi = 5\,\mathrm{MHz}$, as is typical in experiments [21], and such transverse confinement would be able to stabilize linear chains with thousands of ions under an optimized quartic potential. We note that the ion spacing can be made even more uniform by adding higher order multipole potentials.

We now describe quantum gate operations with this large ion chain, mediated by many transverse phonon modes. Given the equilibrium positions of the ions, we can efficiently determine all axial and transverse phonon modes. We then apply a spin-dependent laser force, with the resulting interaction Hamiltonian [22,23]

$$H = \sum_n \hbar\Omega_n(t)\sigma_n^z \cos(kq_n + \mu t), \tag{1}$$

where the transverse displacement q_n of the n-th ion in the x-direction is expressed in terms of phonon modes a_k with eigenfrequency ω_k and the normal mode matrix b_n^k by $q_n = \sum_k b_n^k \sqrt{\hbar/2m\omega_k}(a_k^\dagger e^{i\omega_k t} + a_k e^{-i\omega_k t})$. The normal mode matrix b_n^k and its eigenfrequency ω_k are determined by solving the eigenequations $\sum_n A_{in} b_n^k = \omega_k^2 b_i^k$, where $A_{in} \equiv \partial^2 U/\partial x_i \partial x_n$ are calculated at the ions' equilibrium positions z_i. In eq. (1), σ_n^z is the Pauli spin operator for the n-th ion, $\Omega_n(t)$ denotes the Rabi frequency of the laser pulse on the n-th ion with detuning μ from the qubit resonance, and the effective laser momentum kick k is assumed to be along the transverse x-direction. (For twin-beam stimulated Raman laser forces and hyperfine state qubits, the effective laser kick carries momentum along the difference wave vector $\mathbf{k}_1 - \mathbf{k}_2$ of the two beams.) Due to the strong transverse confinement, the Lamb-Dicke parameter $\eta_k \equiv |k|\sqrt{\hbar/2m\omega_k} \ll 1$, and the Hamiltonian H can be expanded as $H = -\sum_{n,k} \hbar\chi_n(t) g_n^k (a_k^\dagger e^{i\omega_k t} + a_k e^{-i\omega_k t})\sigma_n^z$ with $g_n^k = \eta_k b_n^k$ and $\chi_n(t) = \Omega_n(t)\sin(\mu t)$ (the effect of higher-order terms in the Lamb-Dicke expansion will be estimated later). The corresponding evolution operator is given by [23]

$$U(\tau) = \exp\left[i\sum_{n,k}[\alpha_n^k(\tau)a_k^\dagger + \alpha_n^{k*}(\tau)a_k]\sigma_n^z + i\sum_{m<n}\phi_{mn}(\tau)\sigma_m^z\sigma_n^z \right], \tag{2}$$

where $\alpha_n^k(\tau) = \int_0^\tau \chi_n(t) g_n^k e^{i\omega_k t}\mathrm{d}t$ characterizes the residual entanglement between ion n and phonon mode k and $\phi_{mn}(\tau) = 2\int_0^\tau \mathrm{d}t_2 \int_0^{t_2} \mathrm{d}t_1 \sum_k g_m^k g_n^k \chi_m(t_2)\chi_n(t_1)\sin\omega_k(t_2 - t_1)$ represents the effective qubit-qubit interaction between ions m and n.

For a two-qubit gate on an ion pair i and j, we direct laser light exclusively on these two ions ($\Omega_i(t) = \Omega_j(t) \equiv \Omega(t)$ and all other $\Omega_n(t) = 0$), and the evolution operator reduces to the standard controlled π-phase (CP) gate for $\alpha_n^k(\tau) = 0$ and $\phi_{jn}(\tau) = \pi/4$. For a large ion crystal, the residual entanglement with the motional modes cannot be eliminated completely, but we can minimize the resulting gate infidelity by optimizing the laser pulse shape $\Omega(t)$ [23]. Assuming each phonon mode k is cooled to temperature T_k, the infidelity of the CP gate from the residual motional entanglement is given by $\delta F = [6 - 2(\Gamma_i + \Gamma_j) - \Gamma_+ - \Gamma_-]/8$ [23], where $\Gamma_{i(j)} = \exp[-\sum_k |\alpha_{i(j)}^k(\tau)|^2 \bar{\beta}_k/2]$, $\Gamma_\pm = \exp[-\sum_k |\alpha_i^k(\tau) \pm \alpha_j^k(\tau)|^2 \bar{\beta}_k/2]$, and $\bar{\beta}_k = \coth(\hbar\omega_k/k_B T_k)$.

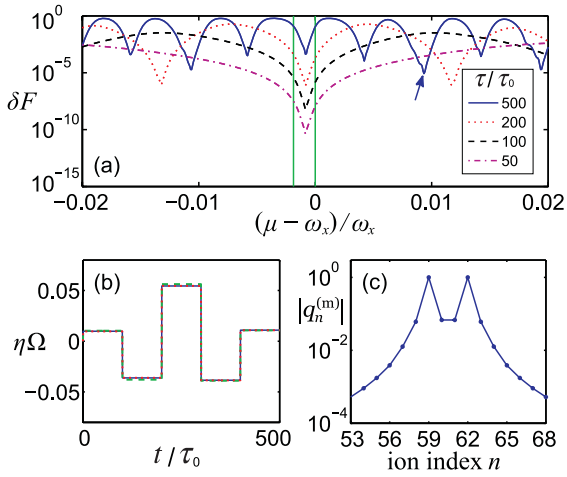

Fig. 3: (Color online) (a) The gate infidelity δF as a function of the laser detuning μ from the qubit resonance, with optimized Rabi frequencies over $M = 5$ equal segments of the laser pulse. Different curves correspond to different gate times. The 120 transverse phonon modes are all distributed within the narrow frequency range indicated by the two vertical lines. (b) The shape of the laser pulse $\eta\Omega$ (in units of ω_x) that achieves the optimal fidelity (with $\delta F = 8.5 \times 10^{-6}$), at the detuning shown by the arrow in (a) (with $(\mu - \omega_x)/\omega_x = 9.3 \times 10^{-3}$) and the gate time $\tau = 500\tau_0$. The dashed (or dotted) lines represent the approximate optimal solutions of the laser shape where only 4 (or 8) ions (from the 59th to 62nd or the 57th to 64th, respectively) are allowed to vibrate and all the other ions are fixed in their equilibrium positions. This approximation does not significantly change the optimal laser pulse shape compared to that of the exact solution (represented by the solid line) where all ions are allowed to vibrate, so the gate is essentially local and the gate complexity does not depend on the crystal size. (c) The relative response of the ions for the gate shown in (b) (characterized by the largest spin-dependent shift $|q_n^{(m)}|$ during the gate time τ). We take a relative unit where $|q_n^{(m)}|$ for the target ions haven been normalized to 1. The fast decay of the response as one moves away from the target ions (59th and 62nd) shows that the gate involves vibration of only local ions.

To minimize the gate infidelity δF, we break the laser pulse on the two ions into uniform segments of constant intensity as shown in fig. 3(b) and optimize the values $\Omega^{(i)}$ $(i = 1, \ldots, M)$ over M equal-time segments [23]. The control of $\Omega(t)$ from one segment to the next can easily be accomplished with optical modulators. (Alternatively, we can modulate the detuning μ of the laser pulse as a control parameter.) After optimization of $\Omega^{(i)}$, the infidelity δF is shown as a function of the detuning μ in fig. 3(a) for $M = 5$ segments. For this example, we perform a CP gate

on the 59th and 62nd ions in this 120-ion chain. With an appropriate choice of $\Omega^{(i)}$ and μ, the infidelity can be made negligible (well below 10^{-5}). For this calculation, we assume Doppler cooling for all modes and take gate times τ in the range $50\tau_0$ to $500\tau_0$, where $\tau_0 = 2\pi/\omega_x = 0.2\,\mu$s is the period of transverse harmonic motion. The gate can certainly be faster with stronger laser beams (there is no speed limit), and with a faster gate, the control becomes easier as the gate becomes more localized (fig. 3).

Interestingly, we use only a few control parameters ($M = 5$ segments) to perform a high-fidelity gate that involves excitation of hundreds of transverse phonon normal modes. This is possible because the gate has a local character where the contribution to the CP gate comes primarily from the spin-dependent oscillations of the ions that are close to the target ions. To show this, we plot the response of each ion in fig. 3(c) during the gate operation. Note that the displacement q_n of the n-th ion is spin-dependent during the gate, and we can use its largest magnitude $|q_n^{(m)}|$ over the gate time τ to characterize the response of ion n, as is shown in fig. 3(c). The ion response decays very fast from the target ions (59th and 62nd in this case) and can be safely neglected after a distance of a few ions. Thus during a gate, only the motion of ions near the target ions are important, and the other ions largely remain in their equilibrium positions. The resultant control parameters from this approximation are almost identical to those shown in fig. 3(b). Owing to the local character of the gate, the complexity of a gate operation does not depend on the chain size, and we can perform gates in parallel on ions in different regions of a large chain.

As we use primarily the quasi-local phonon modes for the gate operations, we assume only local entangling gates where the distance between the target ions is small compared with the length of the whole ion chain. (For distant quantum computing, gate operations can be implemented through aids of a series of mediate local SWAP gates.) Recent studies have shown that with only nearest-neighbor entangling gates in a two-dimensional (2D) lattice, the error threshold for fault-tolerant computation can be still very good, close to the level of one percent [24]. In a one dimensional (1D) ion chain, if we perform gates with distance up to $\sqrt{N}$ (which is still relatively local compared with the size N of the ion chain), this simulates a 2D system, and the error threshold for this case should be as least as good as the 2D case with nearest neighbor entangling gates. Moreover, in the 1D case, it is even possible to perform fault-tolerant quantum computing with only next to nearest-neighbor entangling gates [25], albeit with a more demanding threshold.

We now discuss several sources of noise for gates in a large ion crystal and show that their effects are negligible. First, the axial ion modes have large phonon occupation numbers under Doppler cooling alone, and the resulting thermal spread in position along the axial direction can degrade the effective laser interaction. For example, the lowest axial mode in a 120-ion chain of Yb^+ ions with a spacing $\overline{z} \sim 10\,\mu$m has a frequency of only $\omega_{L0}/2\pi = 9.8\,$kHz and a mean thermal phonon number $\overline{n}_0 \approx \gamma/\omega_{L0} \approx 10^3$ under Doppler laser cooling (radiative half-linewidth $\gamma/2\pi = 10\,$MHz). We assume the quantum gate laser beams are directed along the transverse direction with an axial Gaussian laser profile $\Omega(z) \propto e^{-(z/w)^2}$ centered on each ion. The beam waist is taken as $w = \overline{z}/2.5 \approx 4\,\mu$m so that the cross-talk error probability between adjacent ions is $P_c = e^{-2(\overline{z}/w)^2} < 10^{-5}$. The position fluctuation δz_n of the n-th ion causes the effective Rabi frequency to fluctuate, resulting in a gate infidelity $\delta F_1 \approx (\pi^2/4)(\delta\Omega_n/\bar{\Omega}_n)^2 \approx (\pi^2/4)(\delta z_n/w)^4$. The fluctuation δz_n can be calculated exactly from summation of contributions of all the axial modes and its value is almost independent of the index n for the computational ions (see Appendix). Under Doppler laser-cooling, $\overline{\delta z_n} \approx 0.26\,\mu$m and the corresponding infidelity is $\delta F_1 = 4.4 \times 10^{-5}$. The position fluctuation of the ions may also lead to anharmonic ion motion, whose contribution to the gate infidelity can be estimated by $\delta F_2 \sim (\delta z_n/\overline{z})^2 \sim 6.8 \times 10^{-4}$. Finally, in the transverse direction we estimate the infidelity caused by the higher-order expansions in the Lamb-Dicke parameter. As all the transverse modes have roughly the same frequency $\omega_k \approx \omega_x$, the effective Lamb-Dicke parameter for the transverse modes is $\eta_x = |\Delta\mathbf{k}|\sqrt{\hbar/2m\omega_x} \approx 0.038$ for Yb^+ ions at $\omega_x/2\pi = 5\,$MHz, with each mode containing a mean thermal phonon number $\bar{n}_x \approx 2.0$ under Doppler cooling. The resultant gate infidelity is estimated to be $\delta F_3 \approx \pi^2\eta_x^4(\bar{n}_x^2 + \bar{n}_x + 1/8) \approx 7 \times 10^{-4}$ [19,26]. Note finally that sideband cooling is possible in the transverse direction as all the modes have nearly the same frequency, thus reducing the gate infidelity due to transverse thermal motion by another order of magnitude.

In summary, we have shown through explicit examples and calculations that it is feasible to stabilize large linear ion crystals where the gate complexity does not increase with the size of the crystal and the gate infidelity from thermal fluctuations can be made negligibly small under routine Doppler cooling. The results suggest a realistic prospect for realization of large-scale quantum computation in a simple linear ion architecture.

* * *

This work is supported by IARPA under ARO contract W911NF-04-1-0234W911NF-08-1-0355, the DARPA OLE Program under ARO Award W911NF-07-1-0576, and the MURI Quantum Simulation Program under AFOSR contract. SLZ is supported by the NSF and SKPBR of China.

Appendix: thermal position fluctuation of the ions along the axial direction. – We address individual ions through focused laser beams which typically take a Gaussian shape along the z-direction with $\Omega_n(z) \propto e^{-z_n'^2/w^2}$, where $z_n' = z - z_n$ is centered at the equilibrium position z_n of the n-th ion. Under the Doppler

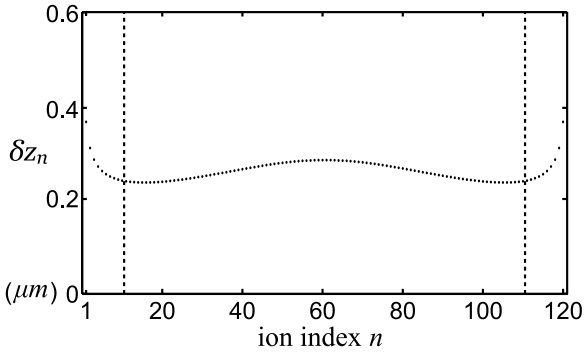

Fig. 4: The axial position fluctuation δz_n is plotted along the ion chain, which is about $0.26\,\mu$m (averaged) for the computational ions (n from 11 to 110).

temperature, the ions have significant thermal fluctuation of their positions along the z-direction, which leads to an effectively fluctuating laser amplitude $\Omega_n(z)$ and induces infidelity to the gate operation. This position fluctuation influences both the single-bit and the two-bit operations in the same way. To quantify the gate error caused by this fluctuation, let us consider a spin-flip gate operated on the n-th ion as a typical example. For a spin-flip with a π-pulse, the gate fidelity is given by $F_1 = \sin^2(\bar{\Omega}_n\tau + \delta\Omega_n\tau) \approx 1 - (\pi^2/4)(\delta\Omega_n/\bar{\Omega}_n)^2$, where $\bar{\Omega}_n$ is the expectation value of the Rabi frequency which satisfies $\bar{\Omega}_n\tau = \pi/2$ for a spin-flip gate, and $\delta\Omega_n$ is its fluctuation caused by the position fluctuation of the ion. From $\Omega_n(z) \propto e^{-z_n'^2/w^2} \approx 1 - z_n'^2/w^2$ around the equilibrium position, the gate infidelity $\delta F_1 \equiv 1 - F_1 = (\pi^2/4)(\delta z_n/w)^4$, where $\delta z_n \equiv \left(\overline{z_n'^4} - \overline{z_n'^2}^2\right)^{1/4}$ characterizes the thermal position fluctuation of the n-th ion along the axial direction.

The phonon modes are in thermal equilibrium under the Doppler temperature T, with their density operator given by $\rho_m = \prod_k \sum_{\{n_k\}} P_k |n_k\rangle\langle n_k|$, where $P_k = \bar{n}_k^{n_k}/(\bar{n}_k+1)^{n_k+1}$ is the probability of having n_k phonons in the k-th mode, and $\bar{n}_k = k_B T/(\hbar\omega_k)$ is the average phonon number. From $\overline{z_n'^2} = \mathrm{tr}(z_n'^2\rho_m)$ and $\overline{z_n'^4} = \mathrm{tr}(z_n'^4\rho_m)$, we explicitly have $\delta z_n = \sqrt{\hbar/2m}\left[\sqrt{2}\sum_k \left(b_n^{z,k}\right)^2 \left(2\bar{n}_k+1\right)/\omega_{z,k}\right]^{1/2}$ where $\omega_{z,k}$ and $b_n^{z,k}$ denote the eigenfrequencies and eigenmatrices of the axial modes. For our example of a 120-ion chain with the Doppler temperature $k_B T/\hbar = 62\,$MHz for the Yb^+ ions, the resultant position fluctuation δz_n is plotted in fig. 4 for all the ions. One can see that for the computational ions (n from 11 to 110), $\delta z_n \approx 0.26\,\mu$m with its value almost independent of the ion index. The position fluctuation is still significantly smaller than the ion spacing ($\approx 10\,\mu$m), which ensures a tiny gate infidelity δF_1 as discussed in the main text.

REFERENCES

[1] Cirac J. I. and Zoller P., *Phys. Rev. Lett.*, **74** (1995) 4091.
[2] Wineland D. J. *et al.*, *J. Res. Natl. Inst. Stand. Technol.*, **103** (1998) 259.
[3] Leibfried D., Blatt R., Monroe C. and Wineland D., *Rev. Mod. Phys.*, **75** (2003) 281.
[4] Blatt R. and Wineland D., *Nature (London)*, **453** (2008) 1008.
[5] Sørensen A. and Mølmer K., *Phys. Rev. Lett.*, **82** (1999) 1971.
[6] Cirac J. I. and Zoller P., *Nature (London)*, **404** (2000) 579.
[7] Milburn G. J., Schneider S. and James D. F. V., *Fortschr. Phys.*, **48** (2000) 801.
[8] García-Ripoll J. J., Zoller P. and Cirac J. I., *Phys. Rev. Lett.*, **91** (2003) 157901.
[9] Duan L.-M., *Phys. Rev. Lett.*, **93** (2004) 100502; Duan L.-M. *et al.*, *Phys. Rev. A*, **73** (2006) 062324.
[10] Sackett C. A. *et al.*, *Nature (London)*, **404** (2000) 256.
[11] Liebfried D. *et al.*, *Nature (London)*, **422** (2003) 412.
[12] Häffner H. *et al.*, *Nature (London)*, **438** (2005) 643.
[13] Leibfried D. *et al.*, *Nature (London)*, **438** (2005) 639.
[14] Moehring D. L. *et al.*, *Nature (London)*, **449** (2007) 68.
[15] Porras D. and Cirac J. I., *Phys. Rev. Lett.*, **96** (2006) 250501.
[16] Schiffer J. P., *Phys. Rev. Lett.*, **70** (1993) 818.
[17] Dubin D. H. E., *Phys. Rev. Lett.*, **71** (1993) 2753.
[18] Kielpinski D., Monroe C. and Wineland D., *Nature (London)*, **417** (2002) 709.
[19] Zhu S.-L., Monroe C. and Duan L.-M., *Phys. Rev. Lett.*, **97** (2006) 050505.
[20] Steane A., *Appl. Phys. B*, **64** (1997) 623.
[21] Kim K. *et al.*, arXiv:0905.0225v1 [quant-ph] (2009).
[22] García-Ripoll J. J., Zoller P. and Cirac J. I., *Phys. Rev. A*, **71** (2005) 062309.
[23] Zhu S.-L., Monroe C. and Duan L.-M., *Europhys. Lett.*, **73** (2006) 485.
[24] Raussendorf R. and Harrington J., *Phys. Rev. Lett.*, **98** (2007) 190504; Svore K. M., DiVincenzo D. P. and Terhal B. M., *Quantum Inf. Comput.*, **7** (2007) 297.
[25] Szkopek T. *et al.*, *IEEE Trans. Nanotechnol.*, **5** (2006) 42; Gottesman D., *J. Mod. Opt.*, **47** (2000) 333.
[26] Sørensen A. and Mølmer K., *Phys. Rev. A*, **62** (2000) 022311.